Supplementary material for: Earth system models overestimate the sensitivity of apparent oxygen utilisation to age change in the deep ocean

*Damien Couespel[a], Xabier Davila[a], Nadine Goris[a], Emil Jeansson[a], Siv K. Lauvset[a], Jerry Tjiputra[a]

[a]NORCE Norwegian Research Centre AS, Bjerknes Centre for Climate Research, Bergen, Norway

Corresponding author: daco@norceresearch.no

Content of this file

Figure S1 to S12 and table S1 to S2.

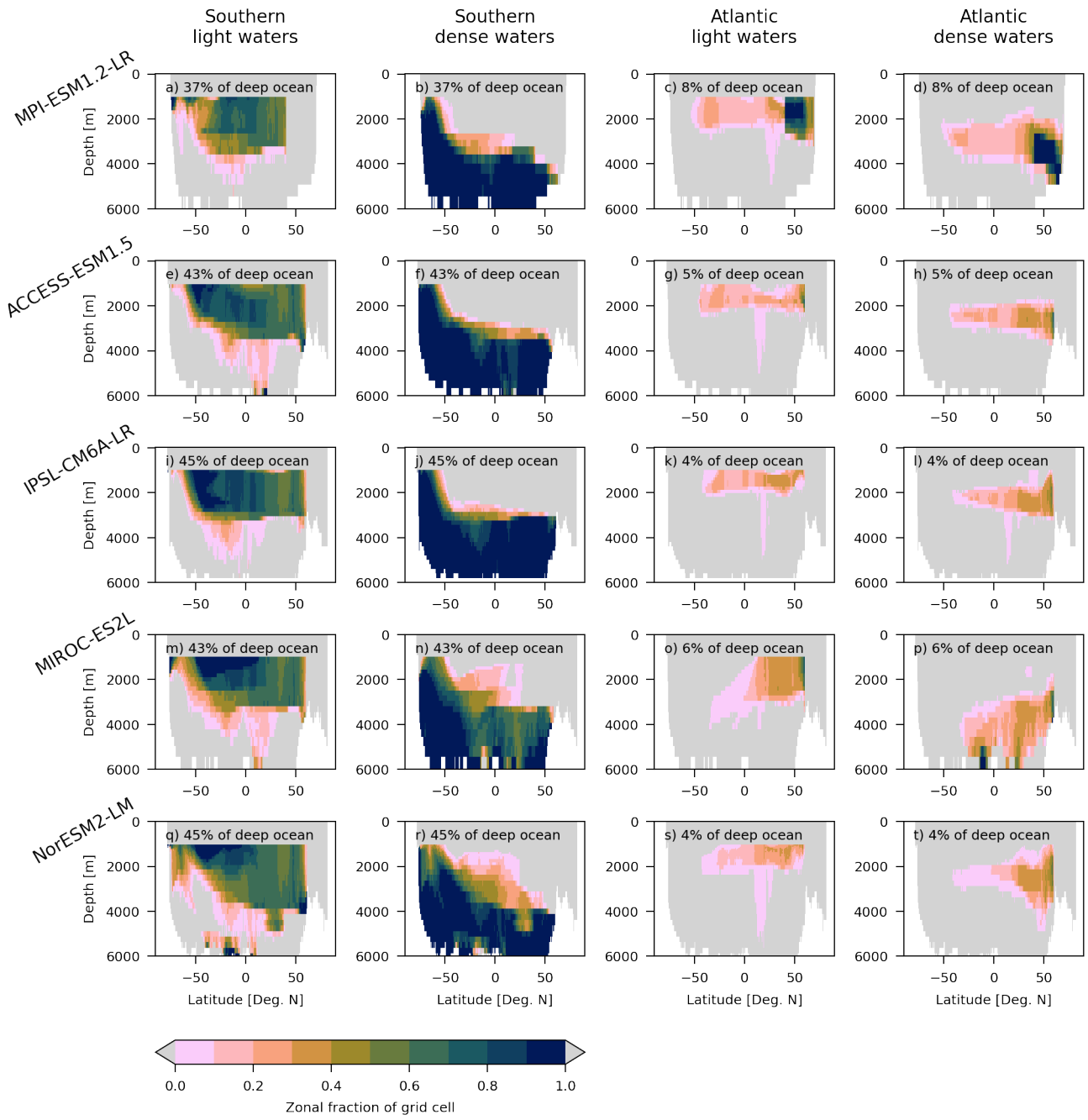

Figure S1. Distribution of the four water-masses - Southern light, Southern dense, Atlantic light, Atlantic dense, from left to right - in the five Earth system models (ESMs): MPI-ESM1.2-LR, ACCESS-ESM1.5, IPSL-CM6A-LR, MIROC-ES2L, NorESM2-LM, arranged from top to bottom. Each depth-latitude sections represent the zonal fraction of grid-cell belonging to the water-mass. For instance, one indicates that all the grid cells zonally belong to the water-mass, while 0.5 indicates that half of the grid cells zonally belong to the water-mass. Areas in grey depict regions where no grid cells are assigned to the water mass. Percentages indicate the fraction of the deep ocean volume covered by each water-mass. The water masses are defined using PO-tracer and density fields averaged over the 1972-2013 period (refer to the methods section in the main manuscript for details).

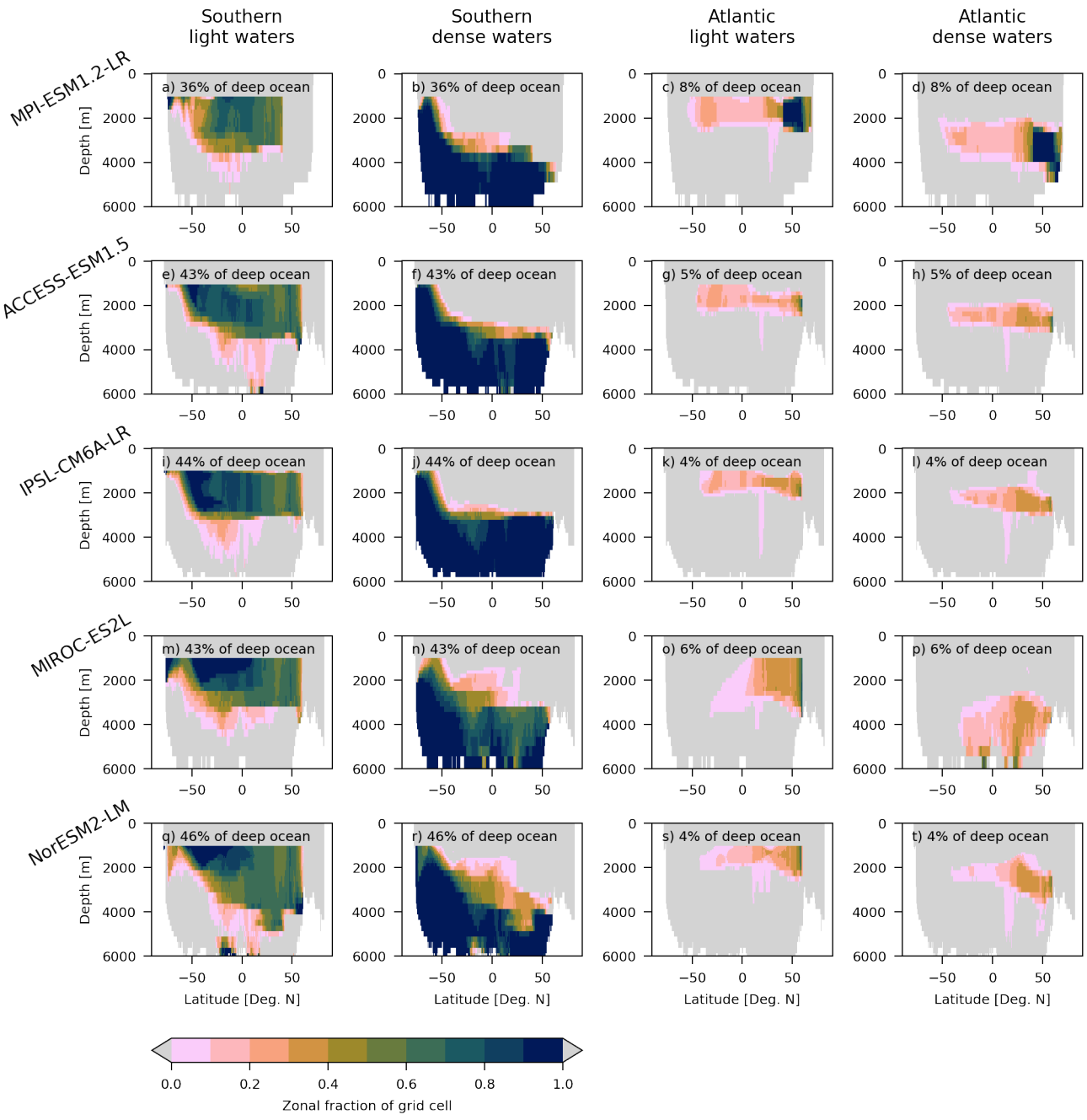

Figure S2. Similar to Fig. S1 but with the water-masses defined using PO-tracer and density fields averaged over the 2050-2099 period: distribution of the four water-masses - Southern light, Southern dense, Atlantic light, Atlantic dense, from left to right - in the five Earth system models (ESMs): MPI-ESM1.2-LR, ACCESS-ESM1.5, IPSL-CM6A-LR, MIROC-ES2L, NorESM2-LM, arranged from top to bottom. Each depth-latitude sections represent the zonal fraction of grid-cell belonging to the water-mass. For instance, one indicates that all the grid cells zonally belong to the water-mass, while 0.5 indicates that half of the grid cells zonally belong to the water-mass. Areas in grey depict regions where no grid cells are assigned to the water mass. Percentages indicate the fraction of the deep ocean volume covered by each water-mass.

Earth system models	Southern dense	Southern light	Atlantic dense	Atlantic light
MPI-ESM1.2-LR	27.78 – 27.71	27.71 – 26.94	27.76 – 27.71	27.71 – 26.86
ACCESS-ESM1.5	27.91 – 27.81	27.81 – 25.88	27.93 – 27.84	27.84 – 26.86
IPSL-CM6A-LR	27.92 – 27.84	27.84 – 27.20	28.90 – 27.81	27.81 – 27.17
MIROC-ES2L	27.65 – 27.48	27.48 – 23.32	27.77 – 27.64	24.64 – 24.11
NorESM2-LM	28.14 – 27.83	27.83 – 26.70	28.16 – 27.93	27.93 – 27.59

Table S1. Range of the potential density anomaly in $\mathrm{kg\,m^{-3}}$ in each water-masses for the 1972-2013 period. The anomaly is relative to a reference pressure of 0 dbar. It is computed with the Gibbs SeaWater (GSW) Oceanographic Toolbox of TEOS-10 in xarray [Caneill and Barna, 2024, McDougall and Barker, 2011]. The Southern and Atlantic water-masses are define based on the PO-tracer (PO^*, Broecker et al. [1991]). Each of these two water-masses is then split into half according to the median of the density distribution. See the method section in the main manuscript for details.

Earth system models	Years of the pi-Control simulation corresponding to years 1850-2099 in the historical and SSPs simulations
MPI-ESM1.2-LR	1850 – 2099
ACCESS-ESM1.5	161 – 410
IPSL-CM6A-LR	1910 – 2159
MIROC-ES2L	1850 – 2099
NorESM2-LM	1600 – 1849
CanESM5	5201 – 5450
CNRM-ESM2-1	1850 – 2099
GFDL-ESM4	101 – 350
UKESM1-0-LL	2250 – 2499

Table S2. Correspondence of years between the pre-industrial control simulation (pi-Control) and the historical and future projections simulations

References

Romain Caneill and Andrew Barna. Gsw-xarray. Zenodo, May 2024.

T. J. McDougall and P. M. Barker. *Getting Started with TEOS-10 and the Gibbs Seawater (GSW) Oceanographic Toolbox*. SCOR/IAPSO WG127, 2011. ISBN 978-0-646-55621-5.

Wallace S. Broecker, Sean Blanton, William M. Smethie Jr., and Gote Ostlund. Radiocarbon decay and oxygen utilization in the Deep Atlantic Ocean. *Global Biogeochemical Cycles*, 5(1):87–117, 1991. ISSN 1944-9224. doi: 10.1029/90GB02279.

Hernan E. Garcia, Zhankun Wang, Courtney Bouchard, Scott L. Cross, Christopher R. Paver, James R. Reagan, Timothy P. Boyer, Ricardo A. Locarnini, Alexey V. Mishonov, Olga K. Baranova, Dan Seidov, and Dmitry Dukhovskoy. World Ocean Atlas 2023, Volume 3: Dissolved Oxygen, Apparent Oxygen Utilization, Dissolved Oxygen Saturation and 30-year Climate Normal. 2024.

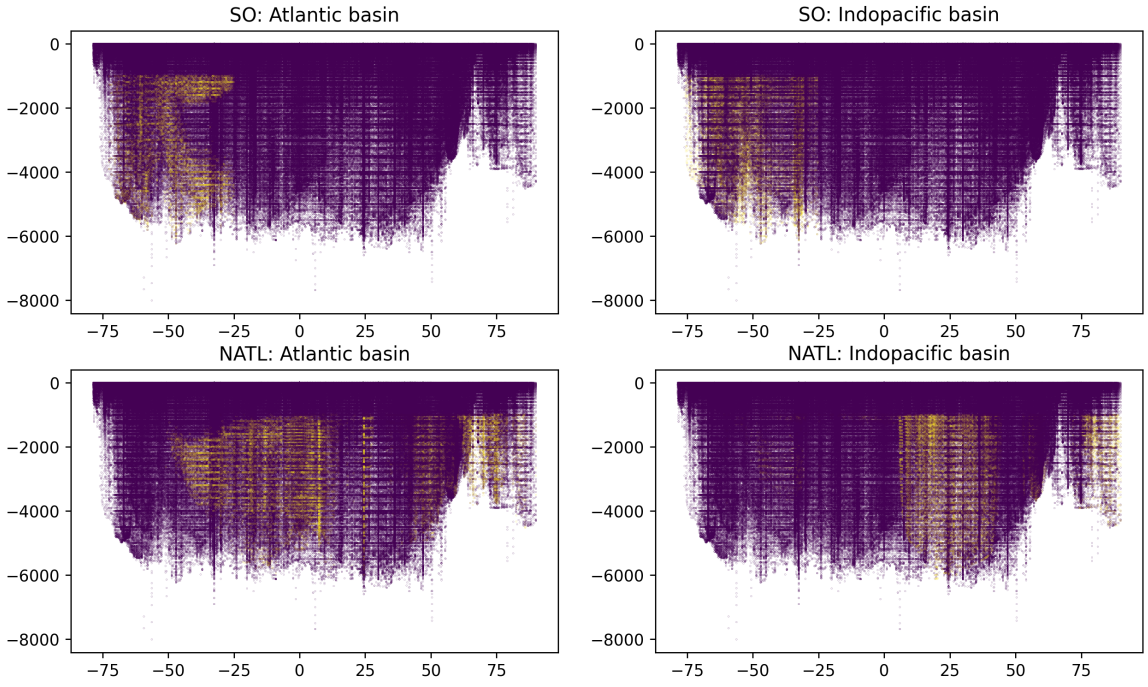

Figure S3. Distribution of the two water-masses based on the observational dataset. The latitude-depth sections in the top row display the Southern dense water-mass, while those in the bottom row show the Atlantic dense water-mass. The left column illustrates the distribution within the Atlantic basin, and the right column the distribution within the Indo-Pacific basin. Yellow dots indicate observational data points that belong to the respective water mass, whereas purple dots represent data points outside of it.

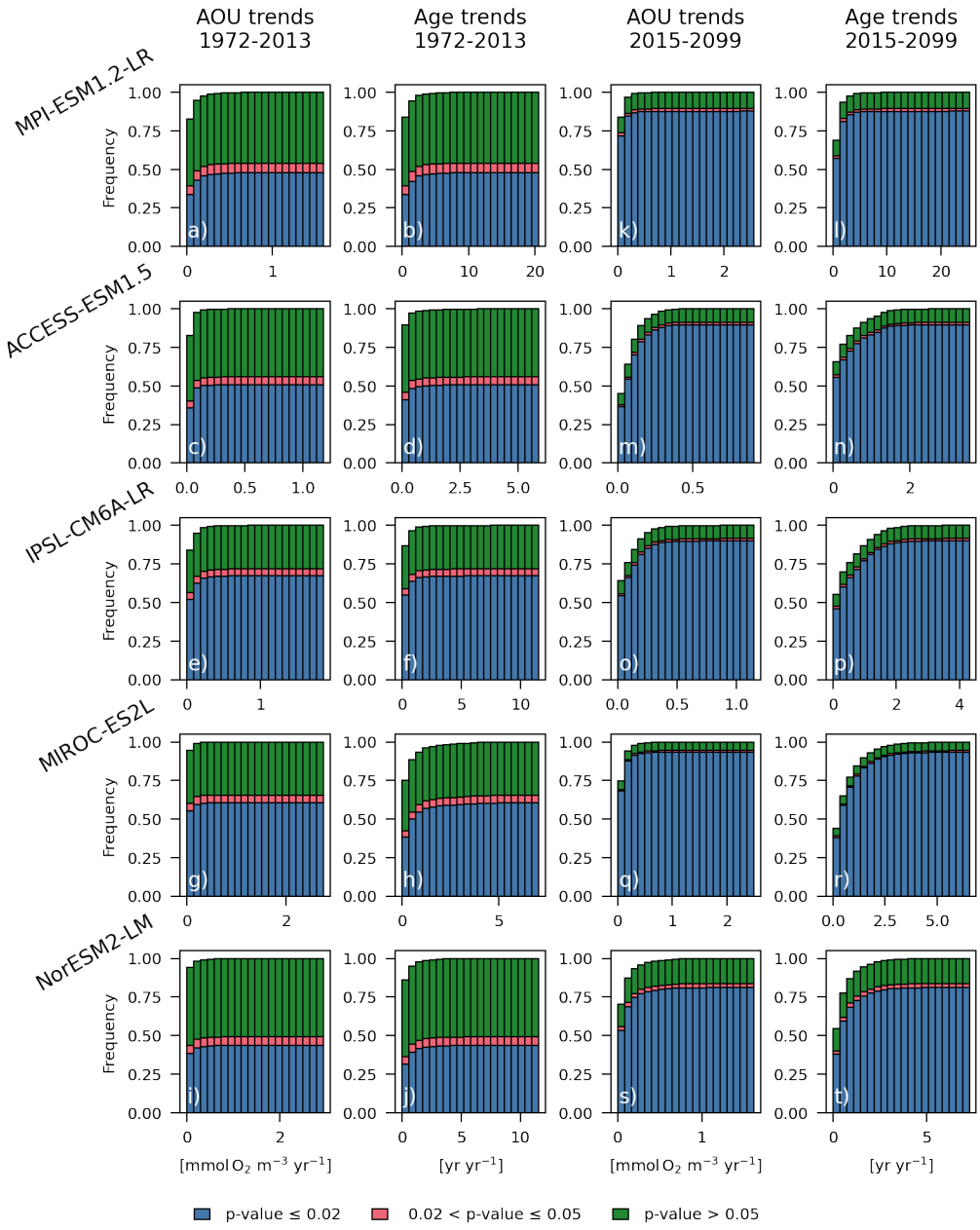

Figure S4. Cumulative histogram of trends in apparent oxygen utilization (AOU) and trends in age for the time periods 1972-2013 and 2015-2099, organized in rows, across five Earth system models (ESMs): MPI-ESM1.2-LR, ACCESS-ESM1.5, IPSL-CM6A-LR, MIROC-ES2L, and NorESM2-LM, listed from top to bottom. The trends are calculated using a linear regression. Each bin shows the frequency of trends, divided into three groups based on p-values: blue represents trends with p-values below 0.02 for both AOU and age; pink represents trends with p-values below 0.05 for both AOU and age but at least one of the two is above 0.02; and green represents trends with p-values above 0.05 for both. We only consider grid-points in the ocean deeper that 1000 m.

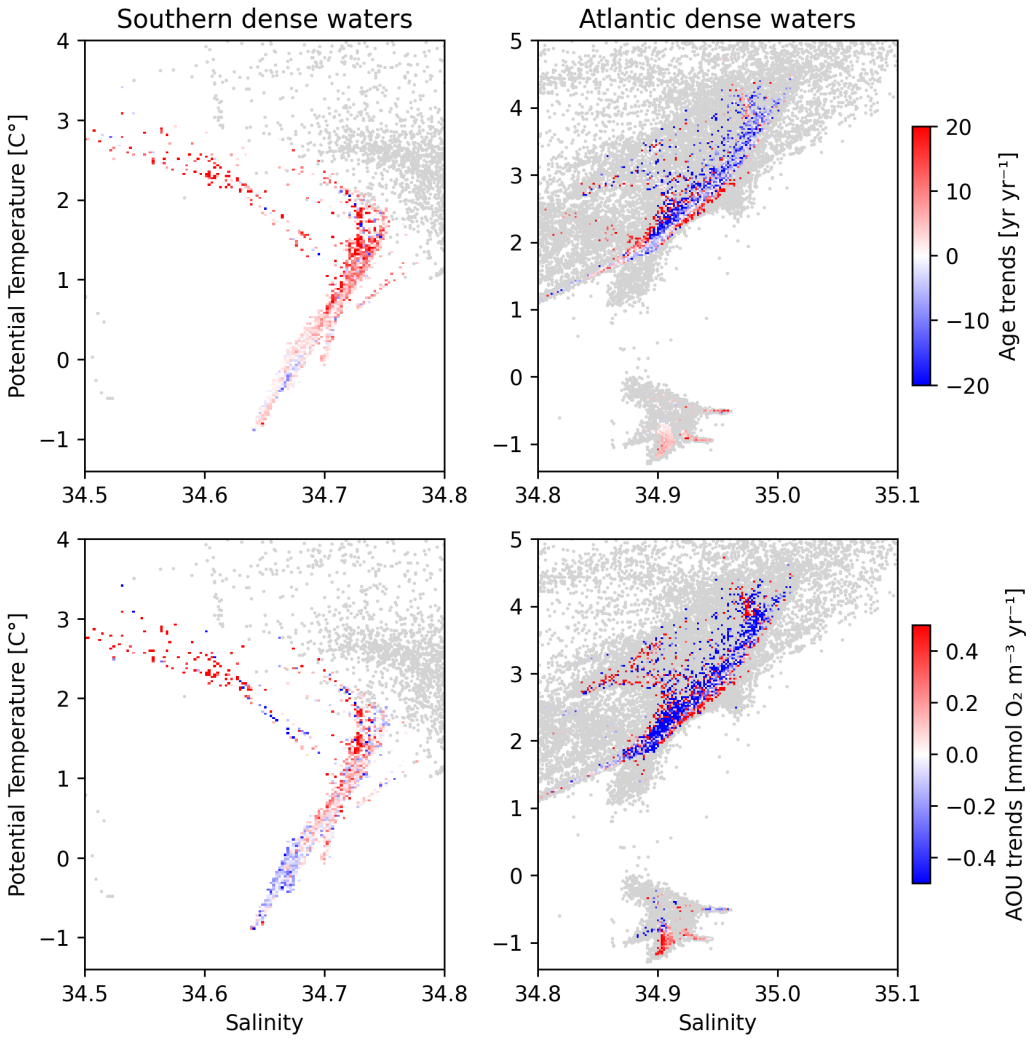

Figure S5. Trends in age (top panels) and trends in apparent oxygen utilization (AOU, bottom panels) over the 1972-2013 period from observational data represented in TS-space. Left panels show the trends in the Southern dense water-mass while the right panels the trends in the Atlantic dense water-mass. Grey shading show the rest of the data not belonging to any of the two water-masses.

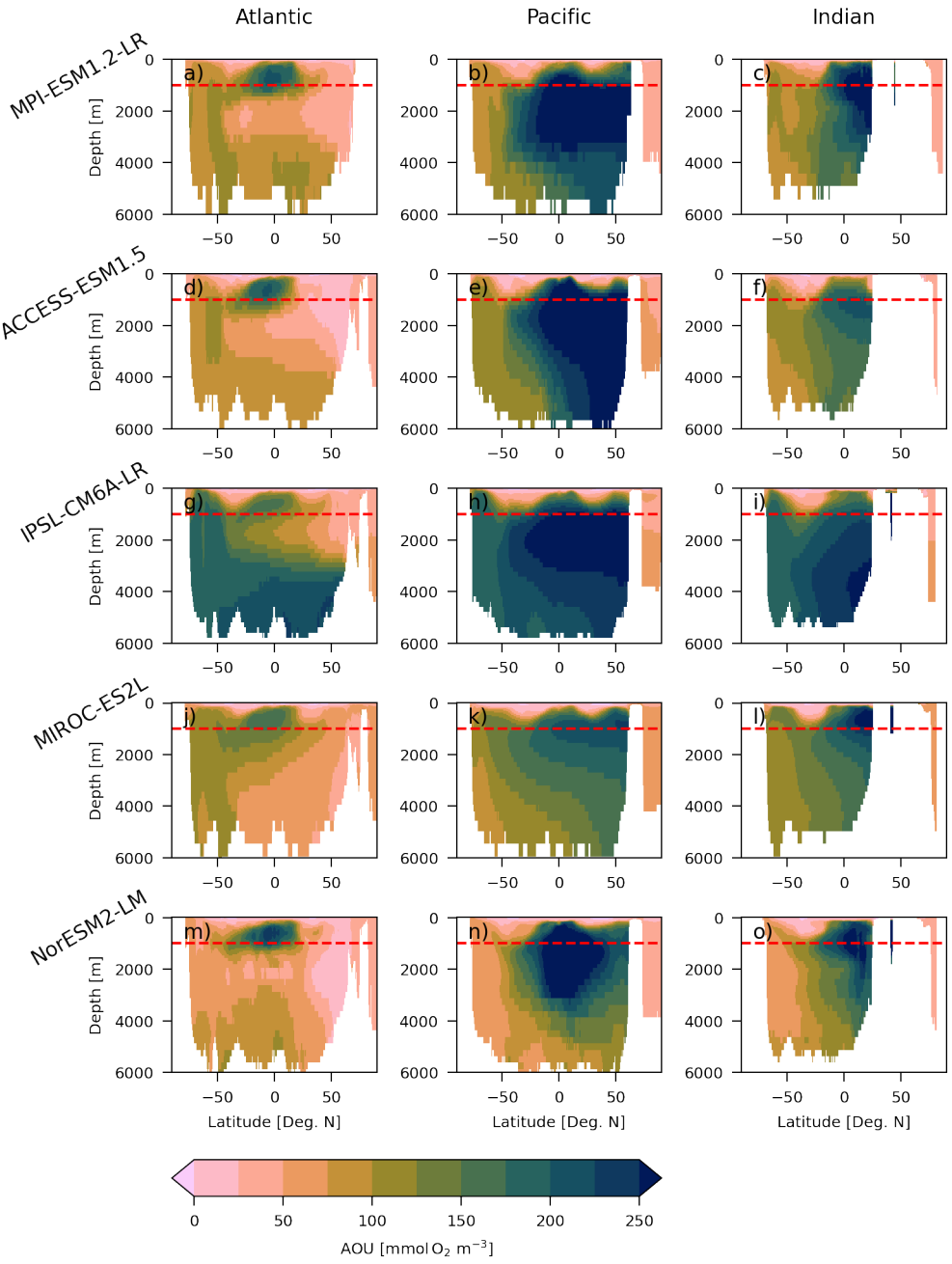

Figure S6. Contemporary (1971-2000) depth-latitude sections of apparent oxygen utilization (AOU) in five Earth system models (ESMs): MPI-ESM1.2-LR, ACCESS-ESM1.5, IPSL-CM6A-LR, MIROC-ES2L, and NorESM2-LM—listed from top to bottom. AOU values are zonally averaged across three ocean sectors: the Atlantic (10°W to 60°W), the Pacific (130°W to 180°W) and the Indian (40°E to 90°E), organized from left to right. The red dashed lines indicate the 1000-meter depth, separating the upper ocean from the deep ocean.

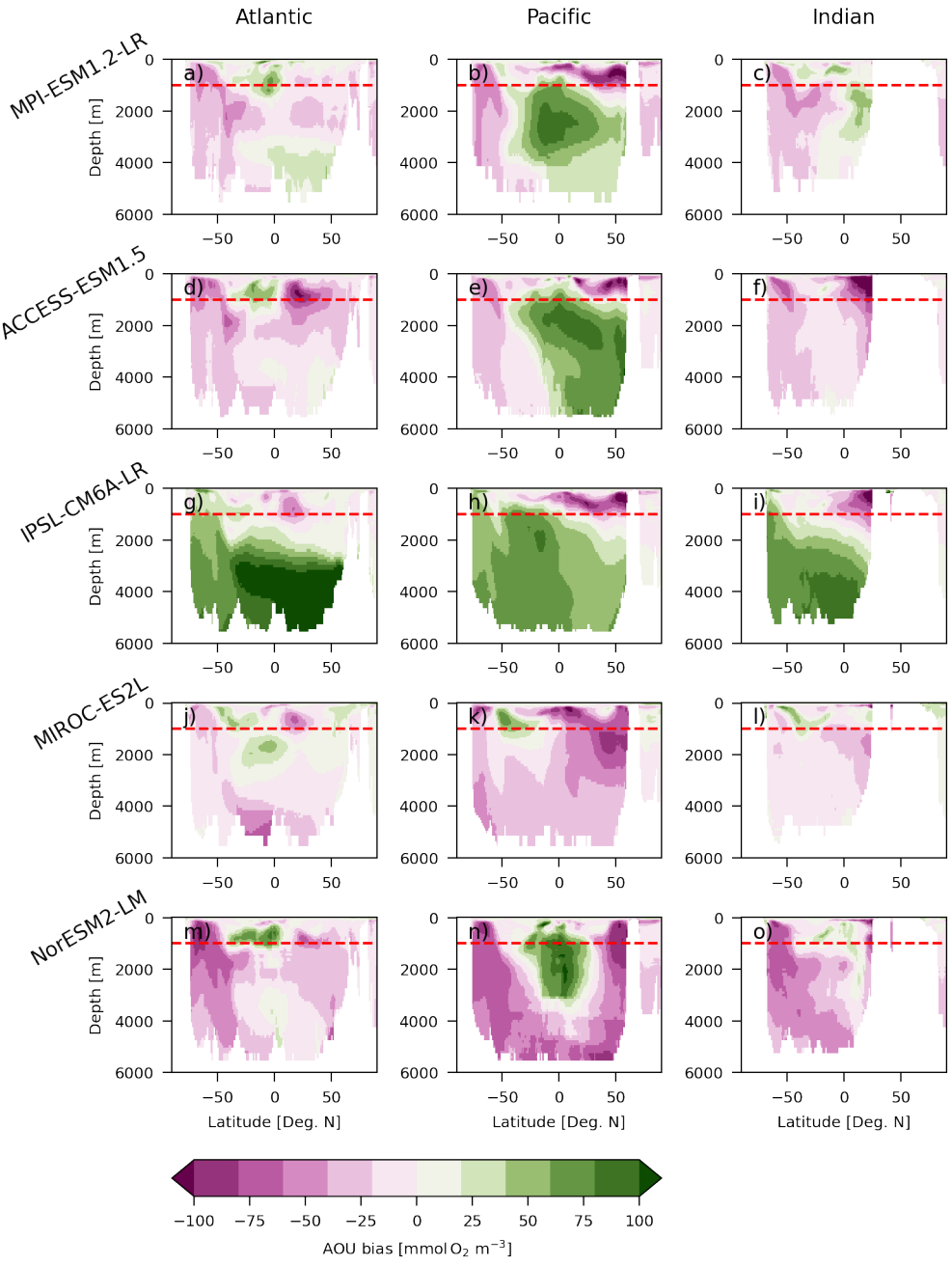

Figure S7. Contemporary (1971-2000) depth-latitude sections of apparent oxygen utilization (AOU) bias against World Ocean Atlas 2023 (WOA23, Garcia et al. [2024]) in five Earth system models (ESMs): MPI-ESM1.2-LR, ACCESS-ESM1.5, IPSL-CM6A-LR, MIROC-ES2L, and NorESM2-LM—listed from top to bottom. AOU bias are zonally averaged across three ocean sectors: the Atlantic (10°W to 60°W), the Pacific (130°W to 180°W) and the Indian (40°E to 90°E), organized from left to right. The red dashed lines indicate the 1000-meter depth, separating the upper ocean from the deep ocean.

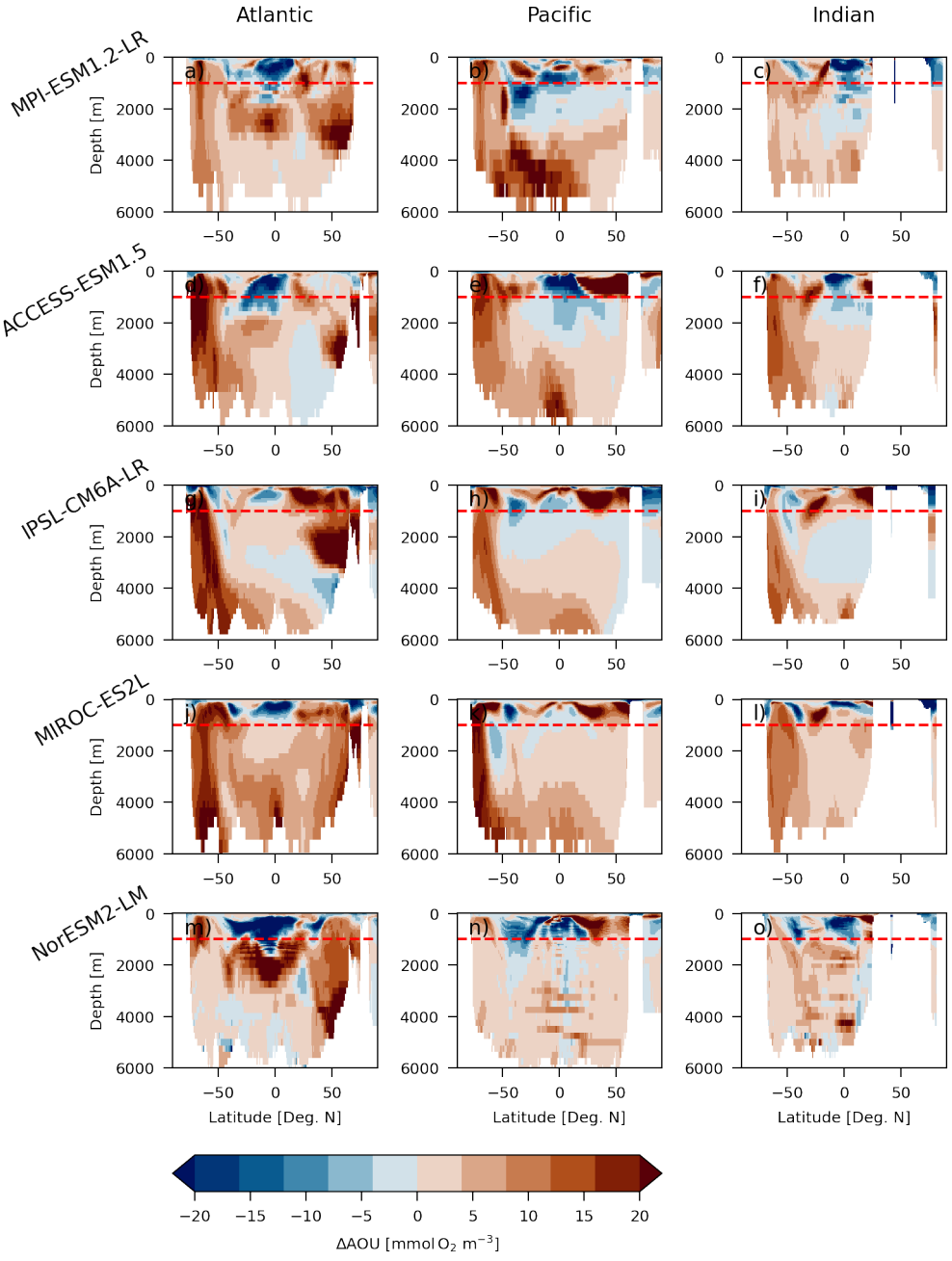

Figure S8. Depth-latitude sections of projected change in apparent oxygen utilization (ΔAOU) under the SSP5-8.5 scenario in five Earth system models (ESMs): MPI-ESM1.2-LR, ACCESS-ESM1.5, IPSL-CM6A-LR, MIROC-ES2L, and NorESM2-LM—listed from top to bottom. ΔAOU is computed as the difference between years 2070-2099 and 1971-2000 and then is zonally averaged across three ocean sectors: the Atlantic (10°W to 60°W), the Pacific (130°W to 180°W) and the Indian (40°E to 90°E), organized from left to right. The red dashed lines indicate the 1000-meter depth, separating the upper ocean from the deep ocean.

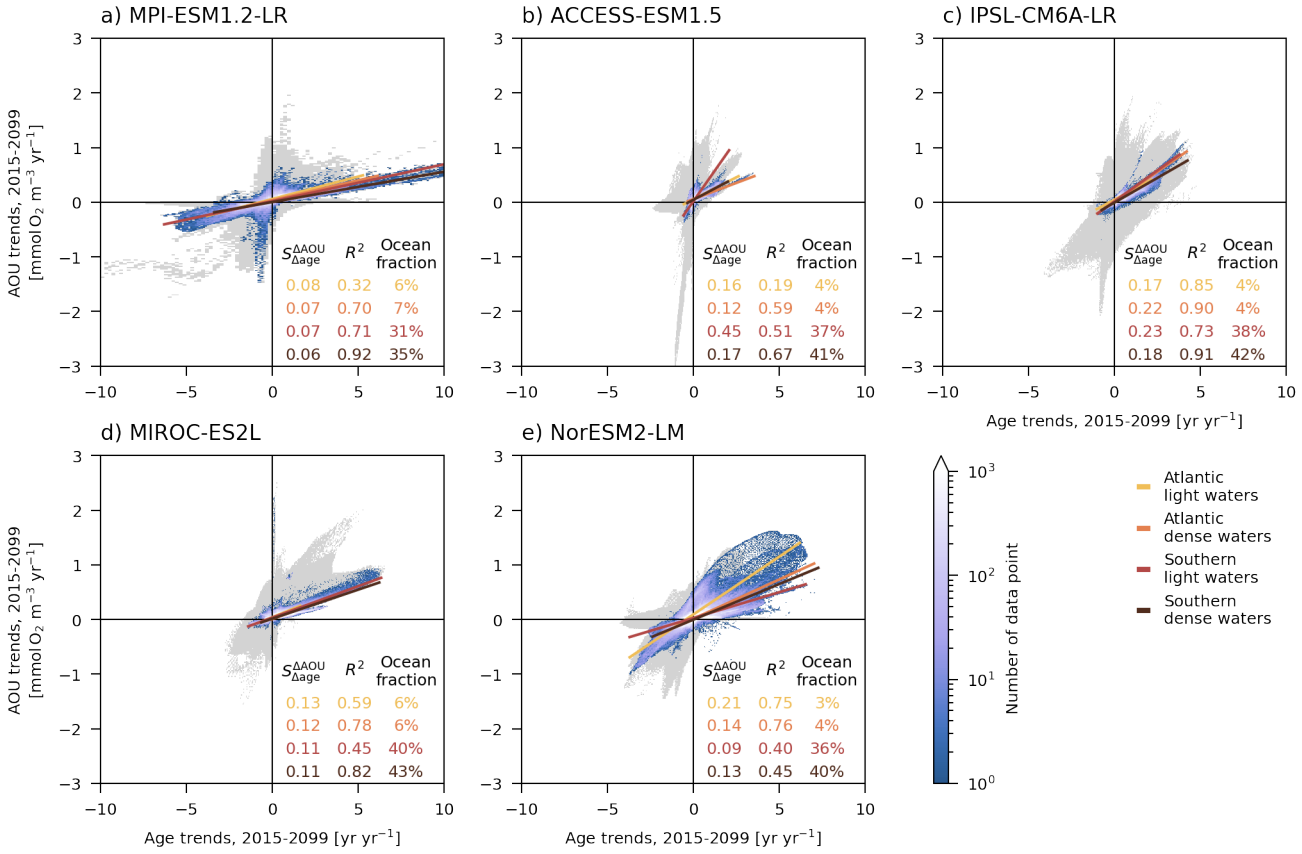

Figure S9. Similar to Fig. 2 in the main manuscript but for the the future period (2015-2099): distribution of the trends in age and trends in apparent oxygen utilization (AOU) simulated with five Earth system models (ESMs): a) MPI-ESM1.2-LR, b) ACCESS-ESM1.5, c) IPSL-CM6A-LR, d) MIROC-ES2L, e) NorESM2-LM. For each ESM the x-axis shows the trends in age and the y-axis the trends in AOU. The trends are computed on years 2015 to 2099 after removing the model drift. The non-significant trends (p-value > 0.05) have been excluded. The blue shading shows the number of data point for each bins of age trends and AOU trends for the Southern and Atlantic light/dense waters. These waters cover the majority of the deep ocean ($>$1000 m), see methods for their definition. A linear regression is computed between the AOU trends and age trends for each water-mass. On each panel, the slope ($S^{\Delta AOU}_{\Delta age}$), the coefficient of determination (R^2) and the fraction of the deep ocean volume are shown in different colors for the 4 different water-masses. The gray shading show the distribution of trends for the entire ocean.

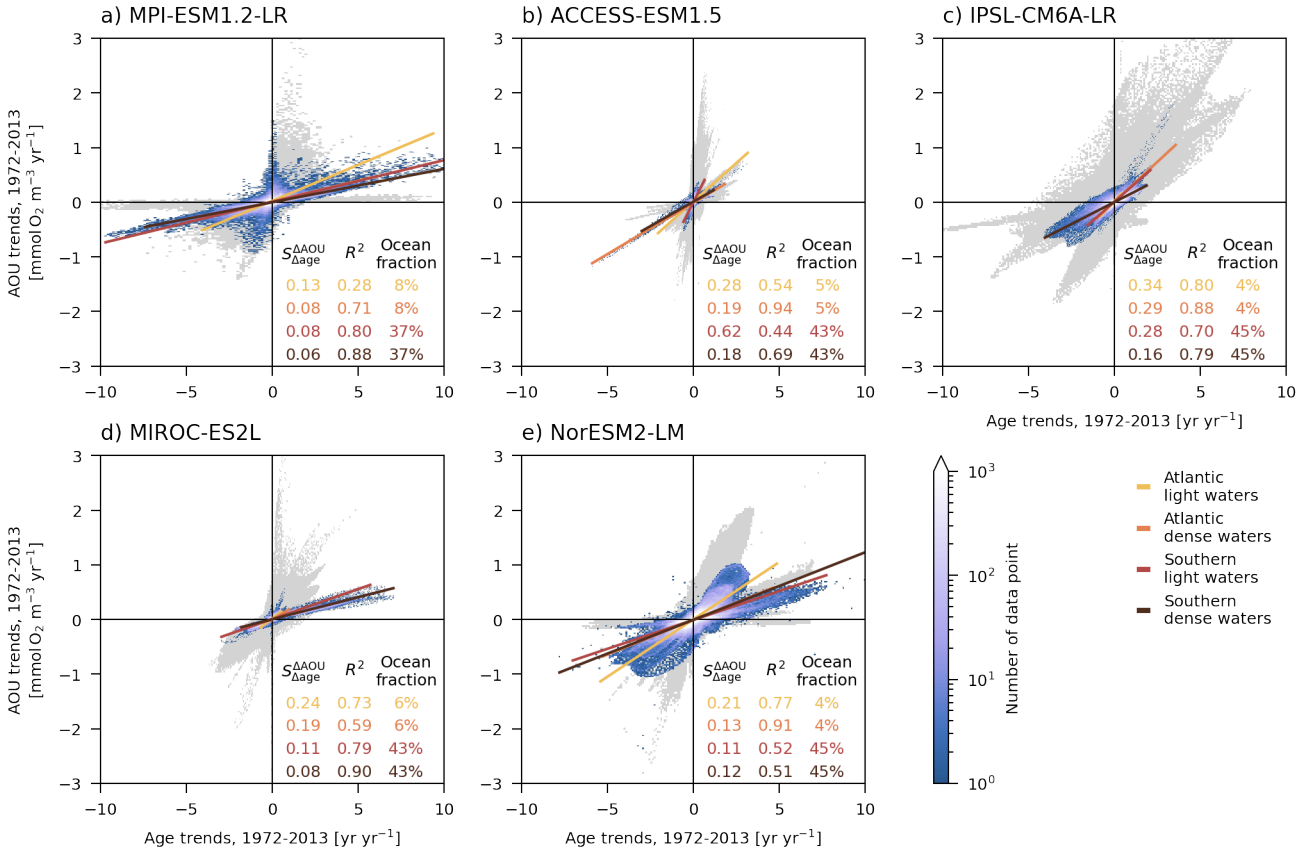

Figure S10. Similar to Fig. 2 in the main manuscript but including trends with low significance (p-value > 0.05): distribution of the trends in age and trends in apparent oxygen utilization (AOU) for the contemporary period (1972-2013) simulated with five Earth system models (ESMs): a) MPI-ESM1.2-LR, b) ACCESS-ESM1.5, c) IPSL-CM6A-LR, d) MIROC-ES2L, e) NorESM2-LM. For each ESM the x-axis shows the trends in age and the y-axis the trends in AOU. The trends are computed on years 1972 to 2013 after removing the model drift. The blue shading shows the number of data point for each bin of age trends and AOU trends for the Southern and Atlantic light/dense waters. These waters cover the majority of the deep ocean (>1000 m), see methods for their definition. A linear regression is computed between the AOU trends and age trends for each water-mass. On each panel, the slope ($S^{\Delta AOU}_{\Delta age}$), the coefficient of determination (R^2) and the fraction of the deep ocean volume are shown in different colors for the 4 different water-masses. The gray shading show the distribution of trends for the entire ocean.

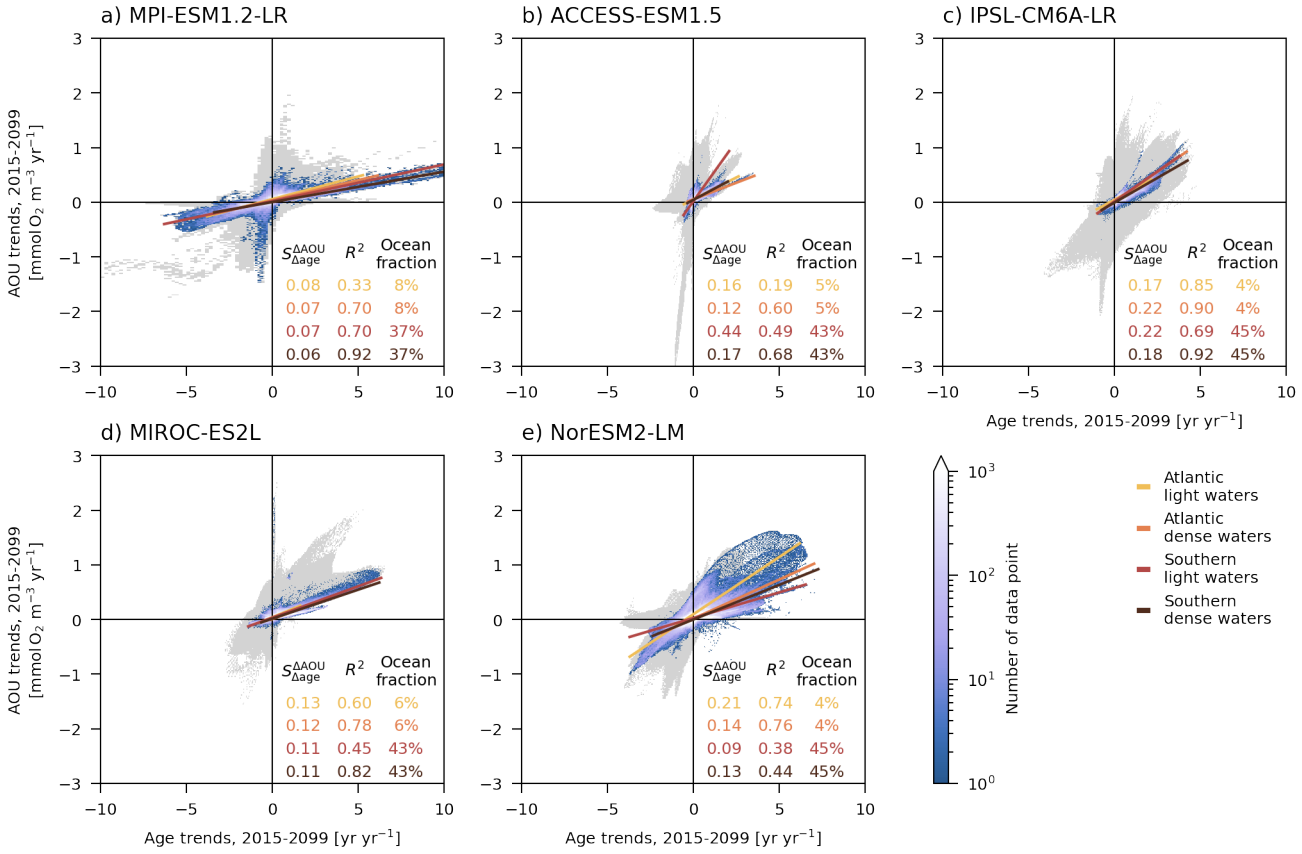

Figure S11. Similar to Fig. S9 but including trends with low significance (p-value > 0.05): distribution of the trends in age and trends in apparent oxygen utilization (AOU) for the future period (2015-2099) simulated with five Earth system models (ESMs): a) MPI-ESM1.2-LR, b) ACCESS-ESM1.5, c) IPSL-CM6A-LR, d) MIROC-ES2L, e) NorESM2-LM. For each ESM the x-axis shows the trends in age and the y-axis the trends in AOU. The trends are computed on years 2015 to 2099 after removing the model drift. The blue shading shows the number of data point for each bin of age trends and AOU trends for the Southern and Atlantic light/dense waters. These waters cover the majority of the deep ocean (>1000 m), see methods for their definition. A linear regression is computed between the AOU trends and age trends for each water-mass. On each panel, the slope ($S^{\Delta AOU}_{\Delta age}$), the coefficient of determination (R^2) and the fraction of the deep ocean volume are shown in different colors for the 4 different water-masses. The gray shading show the distribution of trends for the entire ocean.

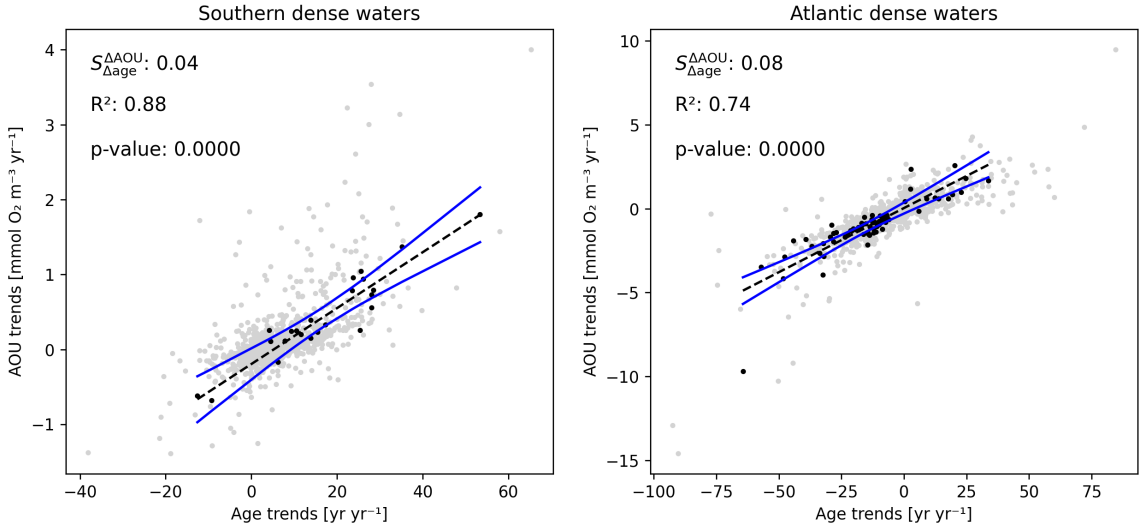

Figure S12. Distribution of the trends in age and trends apparent oxygen utilization (AOU) for the 1972-2013 period from the observational dataset in the Southern dense (left) and Atlantic dense (right) water-mass. For each water-mass, the x-axis shows the trends in age and the y-axis the trends in AOU. A linear regression is computed between the AOU trends and age trends for each water-mass. On each panel, the slope ($S^{\Delta AOU}_{\Delta age}$), the coefficient of determination (R^2) and the p-value of the linear regression are indicated. Only the significant point (in black) are used for the linear regression, the ones in grey are ignored.